Pair Interaction between End-Grafted Polymers onto Spherical Surfaces: A Monte Carlo Study

Juan J. Cerdà, Tomás Sintes,* and Raúl Toral

Departament de Física and IMEDEA (CSIC-UIB), Universitat de les Illes Balears and Consejo Superior de Investigaciones Cientıficas, 07071 Palma de Mallorca, Spain

Received August 28, 2002

ABSTRACT: We present the results of extensive three-dimensional off-lattice Monte Carlo simulations of two interacting spherical brushes. We have measured the interacting force in systems where curvature effects are important. Our results support a description of the force profile divided into two regimes. At short separating distances between the brushes the force is well described by the theory of Witten and Pincus, whereas at larger distances the interaction is reproduced by extending the theory of Flory for dilute polymer solutions. The overall behavior is also compared with the predictions of the phenomenological theory of Doroszkowski and Lambourne. The characteristic radial size of an unperturbed brush follows the same scaling relationship found in the star polymer systems approximation.

I. Introduction

The structure and dynamics of polymer brushes have been the subject of considerable experimental and theoretical activity in the past years. Polymer brushes are characterized by a high concentration of end-grafted polymers onto a nonadsorbing surface. The constrained geometrical environment limits the available space the polymers can occupy, forcing the chains to stretch out, normal to the surface, forming a brush. These systems are found to be particularly relevant in many aspects of polymer science and technology, such as the stabilization of colloidal particles, lubrication, adhesion, or as potential drug carriers.[1−6]

From a theoretical point of view, the scaling properties of polymer chains anchored onto planar surfaces were initially worked out by de Gennes and Alexander.[7,8] Immediately after, Semenov,[9] Milner−Witten−Cates,[10,11] and Zhulina−Priamitsyn−Borisov[12,13] developed a self-consistent-field theory, predicting a parabolic form for the density profile and obtained an expression for the free energy of two interacting flat brushes. Their predictions were well supported by Monte Carlo[14−17] and molecular dynamics[18] simulations.

The introduction of curved interfaces results in polymer brush structures whose properties differ significantly from those at flat interfaces. This is mainly due to the increased volume available to the stretched polymer as it moves away from the interface. These systems are found to display a rich behavior, and for instance, colloidal silica spheres with grafted alkane chains undergo a sol−gel transition when dispersed in hexadecane solution.[19]

More recently, the use of the light-scattering properties of coated spherical particles has been found to be a useful and nondestructive way to probe and size systems ranging from blood cells to paper whiteners.[20] Also, spherical brushes formed by colloidal poly(methyl methacrylate) spheres with a grafted layer of poly(12-hydroxy stearic acid) (PMMA−PHSA) has served as a model to emulate hard spheres, minimizing the effect of van der Waals forces.[21] Therefore, a clear understanding of the polymer induced forces between brushes is essential to precisely determine the effect of polymer additives in chemical and biological systems.

There have been several attempts to determine the rheological properties and the effective interaction between spherical brushes. However, the validity of the results is restricted to specific limiting cases. The monomer concentration profile given by Daoud and Cotton[22] was derived assuming a star-shaped polymer. Witten and Pincus[23] (to be referred as WP) derived an expression for the effective interaction potential in the regime where the chains extend far beyond the diameter of the colloidal particles. More recently, Borukhov and Leibler[24] studied the interaction between spherical brushes in the Derjaguin approximation,[25] whose validity is limited to systems with small curvature effects. Previous Monte Carlo simulations[26] have focused on the density and chain-end profiles of single, noninteracting, brushes.

From the experimental point of view, studies of spherical brushes, and grafted layers in general, appear rather scarce certainly due to the strong difficulties in the control of the grafting procedure with long polymer chains.[27]

The purpose of the present paper is to present the results of extensive numerical simulations of two interacting spherical brushes. The objective is twofold. First, to check, compare, and determine the range of validity of the existing theories, and second, to obtain the interaction profile in the whole range of distances for systems where the curvature effects are relevant. We will show that, when the two particles are brought to a very close distance, the interaction is well described by the WP theory, whereas when the particles are far enough apart, the behavior is reproduced by extending the Flory theory of very dilute polymer solutions.[28] The overall behavior will be also compared with the predictions of the phenomenological theory of Doroszkoeski and Lambourne[29] (to be referred as DL).

The rest of the paper is organized as follows. In section II we present a theoretical review summarizing the main features of the WP theory, the Flory theory for dilute polymer solutions, and the DL theory. In section III we describe the numerical procedure and the

10.1021/ma0213955 CCC: $25.00
Published on Web 01/29/2003

method used to compute the interacting force. In section IV we present a detailed analysis of the numerical calculations, and section V concludes with a brief summary and a discussion of the results.

II. Theoretical Review

We briefly summarize here the main theoretical results concerning the interaction of two spherical brushes, particularly in systems where the curvature effects are important. In such cases, the polymer chain length N is comparable to or even larger than the spherical colloidal radius r_c. The limiting case $N \gg r_c$ will correspond to the star polymer approximation.

Witten and Pincus[23] derived an expression for the free energy of one spherical brush by using the monomer density profile previously obtained by Daoud and Cotton in the star polymer approximation.[22] They assumed that when two colloidal particles, containing each f chains grafted onto their surfaces, were brought together to a very close distance, the system could be approximated by a single colloid with $2f$ polymers anchored onto its surface. Thus, the change in the free energy bringing the two brushes from the infinity to a close distance coincides with the free energy of a single and isolated brush. They found the interaction potential between the two brushes to depend logarithmically on their separation,

$$V_{WP}(R) = A \ln\left(\frac{r_c}{R - 2r_c}\right) \tag{1}$$

where R is the distance between the centers of the colloidal particles. Thus, the force is given by

$$F_{WP}(R) = \frac{A}{R - 2r_c} \tag{2}$$

The constant A was found to follow a power-law dependence with f,

$$A \sim f^{3/2} \tag{3}$$

Since the WP theory is expected to work adequately at small distances, we were interested in finding an expression for the interaction when the spherical brushes are separated by intermediate or large distances. An answer to this problem can be found by extending the Flory theory for dilute polymer solutions.[28]

Flory assumed that for very dilute polymer solutions each polymer can be seen as a collection of monomers forming a rather spherical object characterized by a Gaussian-like monomer density profile. Bringing together two of such polymers might eventually result in an overlapping of the domains. Hence, in the presence of a good solvent, a repulsive force appears between them. The derived expression for the force in units of k_BT takes the form

$$F_F(R) = CR\mathrm{e}^{-DR^2} \tag{4}$$

where the constants C and D scale as

$$C \sim \frac{M^2}{\langle r^2\rangle^{5/2}} \tag{5}$$

and

$$D \sim \frac{1}{\langle r^2\rangle} \tag{6}$$

M is the mass or the total number of segments inside the globular polymer, and $\langle r^2\rangle$ is the averaged end-to-end square distance. We can apply this result to the case of two interacting spherical brushes provided that they are sufficiently apart not to feel the presence of the inner core of the brush. Under these circumstances, we can take $M = Nf$ in the above expression, and $\langle r^2\rangle$ can be defined as twice the averaged square distance of the monomer chain ends forming the brush to the core,

$$\langle r^2\rangle = 2\frac{\int_0^\infty r^2\epsilon(r)\,\mathrm{d}^3\vec{r}}{\int_0^\infty \epsilon(r)\,\mathrm{d}^3\vec{r}} \tag{7}$$

where $\epsilon(r)$ is the chain-end monomer concentration.

A completely different approach to the study of the interaction between two spherical brushes was given by the phenomenological theory of Doroszkoeski and Lambourne.[29] They assumed that as the two spherical brushes approach, the polymer chains do not interpenetrate, resulting in an increase of the local monomer concentration and, as a consequence, in the osmotic pressure. The originated repulsive force is given by the change in the osmotic pressure multiplied by the contact area between the two brushes:

$$F_{DL}(R) = \Delta\Pi\pi\left(R_0 - \frac{R}{2}\right)\left(R_0 + \frac{R}{2}\right) \tag{8}$$

where R_0 is the characteristic radial size of an unperturbed brush measured from the center of the core. $\Delta\Pi$ is the change of the osmotic pressure, and it is given by a rather complicated function of the size of the interacting region. In units of k_BT it reads

$$\Delta\Pi = \frac{1}{v_1}\left(\frac{{v^*_2}^2 - {v_2}^2}{2} + \frac{{v^*_2}^3 - {v_2}^3}{3} + \mathcal{O}({v_2}^4)\right) \tag{9}$$

where v_2 is the volume fraction occupied by the Nf monomers in an isolated brush:

$$v_2 = \frac{aNf}{\tau} \tag{10}$$

a being the volume of a single monomer and τ the volume occupied by the monomer chains:

$$\tau = \frac{4\pi}{3}({R_0}^3 - {r_c}^3) \tag{11}$$

v^*_2, defined by

$$v^*_2 = v_2(V_R + V_H)/V_H \tag{12}$$

is the volume fraction occupied by the monomers in the compressed state. Monomers initially located inside V_R (half of the overlapping region between the two brushes) are redistributed into the volume V_H since chains are not allowed to interpenetrate in this model[32] (see Figure 1). Finally, v_1 is a constant giving the molar volume of the solvent.

The DL theory is, in principle, valid over all relative distances between the two brushes. However, a quantitative analysis of this model involves a truncated expansion of the change in the osmotic pressure and

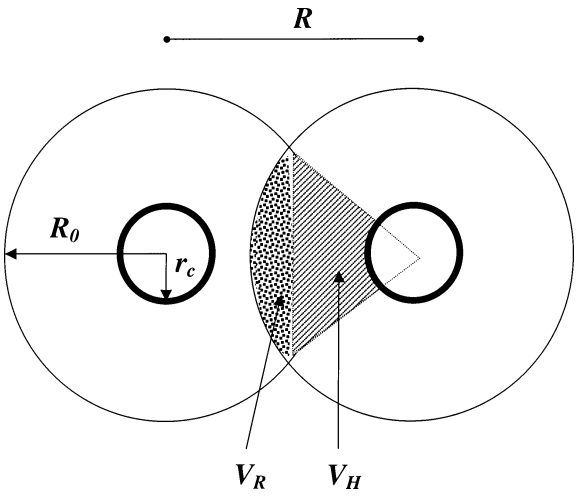

Figure 1. Schematic representation of two interacting spherical brushes in the DL model. R_0 is the radial size of an isolated brush, and r_c is the core radius. The shadowed regions represent V_H and V_R.

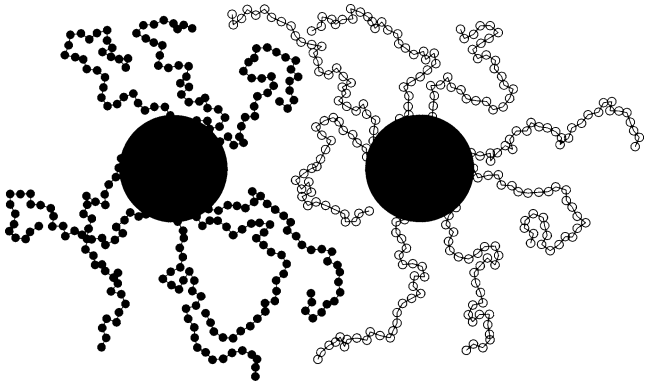

Figure 2. Schematic representation of two spherical brushes separated a distance R. Each brush consists of f polymers of length N grafted to a spherical surface of radius r_c.

requires the determination of the unperturbed radial size of the brush R_0 which is usually difficult to measure with precision.

In the next section we will introduce the numerical model the purpose of which is to compute the force between two spherical brushes. The results obtained will serve to test, compare, and determine the range of applicability of the WP, Flory, and DL theories.

III. Numerical Model

We have simulated the interaction between two spherical brushes by using three-dimensional off-lattice Monte Carlo methods.[26] A brush is generated by homogeneously distributing f polymer chains onto a colloidal particle modeled by a impenetrable sphere of radius r_c. Each polymer is represented by the *pearl-necklace model*[30] containing N beads of diameter σ. The initial configuration of the self-avoiding polymer is randomly generated being the first monomer permanently anchored to the surface. (It is never allowed to move.) A schematic representation of the system is shown in Figure 2.

Monomers interact through a steric hard-core potential of the form

$$U_{\text{steric}} = \sum_{i,j=1}^{2\times N\times f} V(r_{ij}) \tag{13}$$

where V is a hard-sphere potential:

$$V(r_{ij}) = \begin{cases} 0, \text{ for } |\mathbf{r}_i - \mathbf{r}_j| > \sigma \\ \infty, \text{ for } |\mathbf{r}_i - \mathbf{r}_j| < \sigma \end{cases} \tag{14}$$

Different polymer configurations are generated by changing the position of a randomly selected monomer. If the monomer is inside the chain (between the first monomer, permanently anchored, and the last monomer), its position changes by rotating an arbitrary angle between 0 and 2π around the axis connecting the previous and following monomer in the chain. Chain ends just perform random wiggling motions. The proposed motion is accepted whereas the excluded-volume interaction is preserved. A link-cell method[31] has been implemented in the algorithm to efficiently check all possible monomer overlaps.

Initially, the two spherical brushes are kept sufficiently far away to ensure that during the equilibration process they do not interact. The simulation box is taken to be large enough to avoid any possible boundary effects.

We define one Monte Carlo step (MCS) as $2 \times N \times f$ trials to move the chains. Initially, each individual spherical brush has been equilibrated typically during 2×10^6 MCS.

To compute the force between the two spherical brushes, we have used the numerical technique developed by Toral, Chakrabarti, and Dickman.[16]

The main idea consists of computing the change in the free energy $\mathcal{F}$ due to an infinitesimal change in the relative positions R of the two interacting spherical brushes. The force, in units of k_BT, is given by

$$F(R) \equiv \frac{\partial \ln Z(R)}{\partial R} \tag{15}$$

where $Z(R) = \exp(-\mathcal{F}k_BT)$ is the partition function of the system. Because of the hard-core structure of the potential (see eq 14), the partition function

$$Z(R) = \int \prod_{i=1}^{2\times N\times f} \mathrm{d}r_i \exp\Big(-\sum_{j=1}^{2\times N\times f} V(r_{ij})/k_BT\Big) \tag{16}$$

is equal to the volume of all possible polymer chains configurations compatible with the two spherical colloids separated a distance R. The force is finally obtained by numerically evaluating the averaged sum over all i monomers of a polymer belonging to brush A and a monomer j of brush B located within a distance $r < r_{ij} < r + \Delta r$ and forming an angle $\theta < \theta_{ij} < \theta + \mathrm{d}\theta$ measured with respect to the line that joins the two colloids.

$$F(R) = \left\langle \frac{1}{\Delta r} \sum_{i=1}^{N\times f} \sum_{\substack{j=1 \\ r<r_{ij}<r+\Delta r}}^{N\times f} \cos\theta_{ij} \right\rangle \tag{17}$$

The procedure starts by placing the two equilibrated brushes at a large enough value of the distance R. After the force has been computed by using the above expression, the distance R is reduced by an amount $\Delta R = 1$, and the system is let to equilibrate further by 10^5 MCS, before computing the force again. The whole process is repeated until the desired minimum value of the distance R is achieved. $\Delta r = 0.001$. Additionally, a similar expresion for the interactions between the

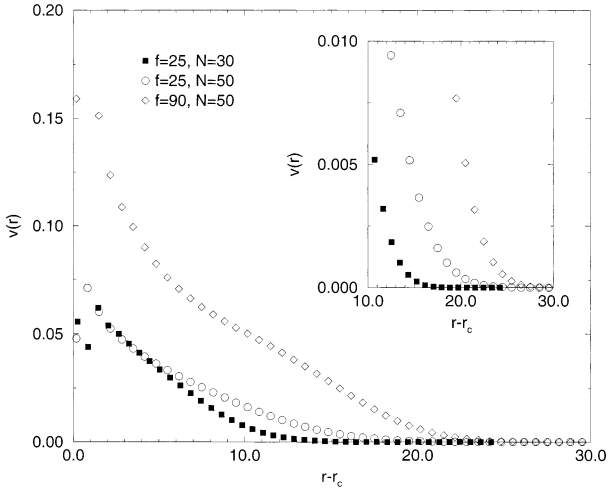

Figure 3. Volume fraction occupied by the monomers $v(r)$ plotted against the distance to the surface core $r - r_c$ for different values of the chain length N and number of grafted chains f. Inset: zoom of the region where $v(r)$ drops to zero, defining the characteristic size of the brush R_0.

monomers and the colloidal particle cores has to be considered to compute the whole force between the two brushes.

IV. Results and Discussion

The force between two spherical brushes has been computed as a function of their relative distance for different sets of parameters (N, f). The core radius of the colloidal particle where polymers are grafted is taken to be $r_c = 5\sigma$ and is kept constant through all the simulations. The diameter of the monomers is set to $\sigma = 1$. We have varied the number of grafted chains from $f = 5$ to $f = 90$, and we have taken polymer chain lengths in the range $N = 30$ to $N = 100$.

To compare the numerical results with the theoretical predictions of the DL theory, we need to determine the characteristic radial size of an unperturbed spherical brush R_0. This quantity is defined as the value of r where the monomer radial density profile $\phi(r)$ drops to zero. $\phi(r)$ is defined as usual:

$$\phi(r) = \frac{\nu(r)}{4\pi r^2 \, \mathrm{d}r} \tag{18}$$

$\nu(r)$ being the number of monomers located within a distance between r and $r + \mathrm{d}r$ from the center of the sphere (to this purpose we have taken $\mathrm{d}r = \sigma/2$). As an example, in Figure 3 we have plotted the volume fraction occupied by the monomers $v(r) = 4\pi/3(\sigma/2)^3\phi(r)$ for different values of chain length N and number of grafted chains f.

In agreement with the results of Toral et al.,[26] we have found that $R_0(N,f)$ behaves as in the star polymer approximation, reproducing the scaling relationship

$$R_0 \sim N^{3/5} f^{1/5} \tag{19}$$

This result supports the previous findings of Daoud and Cotton[22] expected to be valid for large polymer chains ($N \gg r_c$) and a large number of grafted chains. In Figure 4 the brush height R_0 is represented as a function of $x = N^{3/5} f^{1/5}$. Note that all the data fall reasonably well on a straight line of unitary slope. As a consequence, since the WP free energy was derived under the assumption of star polymer monomer density profile, we can expect the WP theory to work properly when the two brushes are in close proximity.

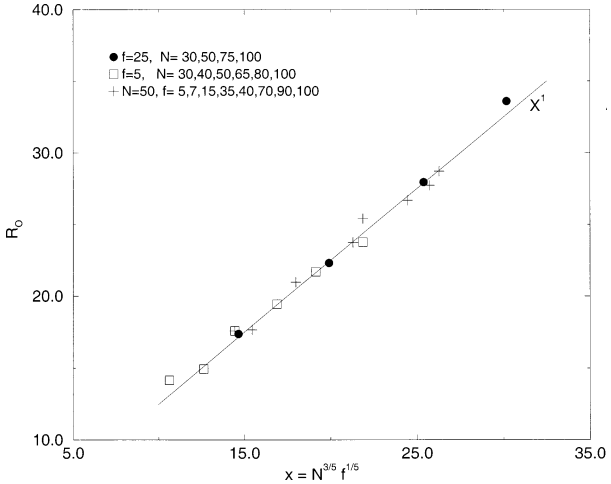

Figure 4. Brush height R_0 as a function of $x = N^{3/5} f^{1/5}$. The straight line of unitary slope corresponds to the star polymer approximation.

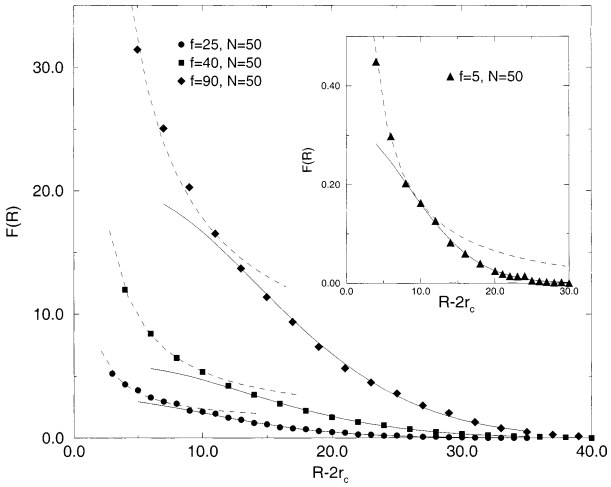

Figure 5. Force between two interacting spherical brushes for $N = 50$ and $f = 25$, 40, 90. Inset plot: case $N = 50$, $f = 5$. At small relative distance the data are fitted according to the WP theory (dashed curves), whereas at larger distances the force profile is reproduced by the Flory theory (solid lines).

The computed force between the two brushes vs their relative distance is represented in Figure 5. We have taken a chain length of $N = 50$ and varied the number of chains $f = 5$, 25, 40, 90. At short distances the interacting profile can be fitted according to the WP theory (dashed curve), whereas at larger distances the measured data can be adjusted with the Flory-type theory introduced above for dilute polymer solutions (solid curve). Figure 6 shows the results for $f = 25$ and chains lengths $N = 30$, 50, 100. Notice that at small distances the force profile becomes rather independent of N as expected from the WP theory. As can be seen in the previous plots, and in all the cases studied, it is remarkable that with the WP and Flory theories in principle valid in the limiting cases of small and large relative distance between the brushes, we can adjust the whole interacting profile.

The best fit to the numerical data determines the values of the adjustable constants A (see eq 2) and C and D (see eq 4) that appear in the WP and Flory theories, respectively. The behavior of A, for $N = 50$, as

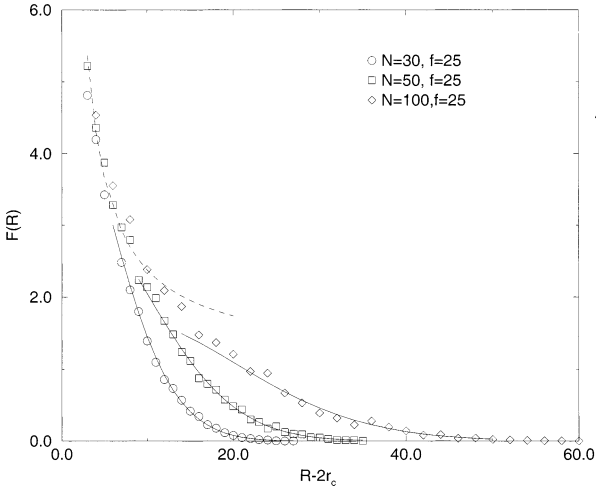

Figure 6. Same as Figure 5 for $f = 25$ and $N = 30$, 50, 100.

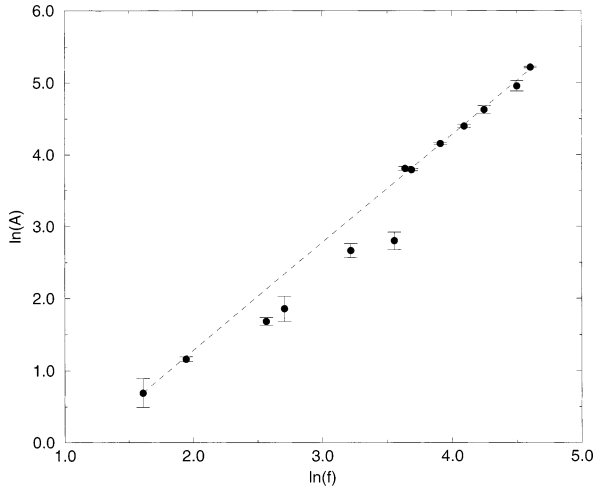

Figure 7. A log−log plot of the parameter A vs the number of grafted chains f. The best fit to the data gives a slope of 1.50 ± 0.02, in agreement with the expected power-law behavior of $^3/_2$ (see eq 3).

a function of the number of grafted chains f is represented in a log−log plot in Figure 7. The best fit to the data gives a slope of 1.50 ± 0.02, in agreement with the expected power-law dependence $A \sim f^{3/2}$ (see eq 3). We should remark that the WP theory was derived in the limiting cases of $f = 1$, $f = 2$, and $f \gg 1$. This fact explains the small deviations observed from the expected theoretical behavior for the intermediate values of f ($15 \leq f \leq 25$). In Figure 8, we show in a log−log plot the scaled force $F(R)/f^{3/2}$ as a function of the relative distance between the brushes. We can observe all the data falling into a master curve for small distances where the WP theory is expected to work. Deviations appear as soon as we enter in the Flory regime. For the sake of clarity, we have drawn a line with slope −1 that is followed by the numerical data in the WP regime.

To analyze the behavior of parameters C and D, we need to compute the averaged square distance of the chain-end monomers as it has been described in eq 7. The chain-ends concentration $\epsilon(r)$ is defined similarly to eq 18 as

$$\epsilon(r) = \frac{\mu(r)}{4\pi r^2 \, \mathrm{d}r} \tag{20}$$

$\mu(r)$ being the number of chain-end monomers within a distance between r and $r + \mathrm{d}r$.

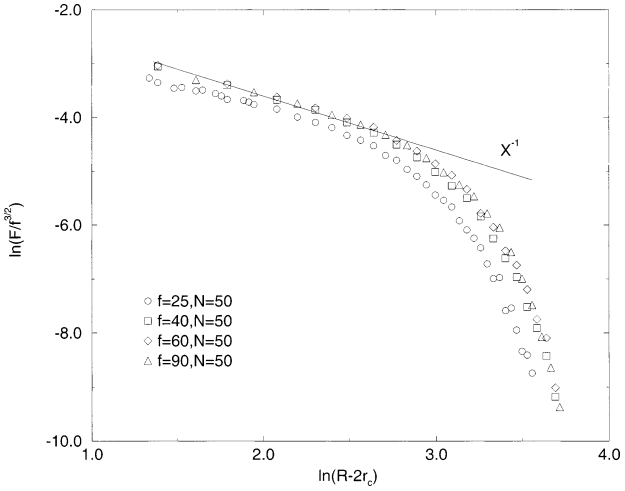

Figure 8. A log−log plot of $F/f^{3/2}$ as a function of the relative distance between brushes $R - 2r_c$. A solid line of slope −1 is included to guide the eye and identifies the WP regime.

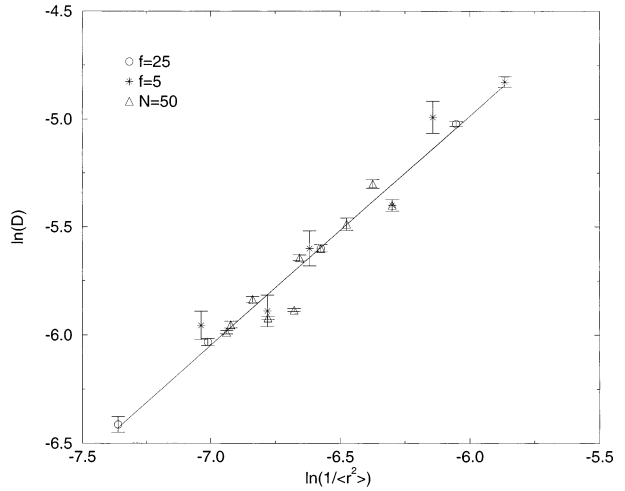

Figure 9. A log−log plot of the constant D vs the inverse of the averaged square distance of the chain-end monomers $1/\langle r^2 \rangle$. The best fit to the data gives a slope of 1.06 ± 0.05 supporting the expected linear relationship of eq 6.

The behavior of D as a function of $1/\langle r^2 \rangle$ for all the sets (N, f) studied is shown in Figure 9. The best fit to the data gives a slope of 1.06 ± 0.05, in agreement of the expected linear relationship (see eq 6).

Similarly, we have plotted in Figure 10 on a log−log scale $C/(Nf)^2$ vs $1/\langle r^2 \rangle$. For the sake of clarity, we have included a solid line of slope $^5/_2$ corresponding to the theoretical prediction of Flory (see eq 5). Deviations from this behavior are found in systems with large f and small N values, precisely where the assumption of a Gaussian monomer density profile fails. In the first case, large f values force the chains to be strongly stretched, whereas small chain lengths fall out of the asymptotic regime where the Gaussian distribution for a globular polymer is found.

There are two main reasons for the Flory theory to break down. First, the density profile of end-grafted polymer chains is not Gaussian, in general, except for highly curved surfaces. The latter case corresponds to the star polymer approximation where the center-to-end distance is found to reproduce a Gaussian distribution.[33] Furthermore, the theory does not consider the changes induced in the density profile while the polymers interact. Second, when two brushes are far enough,

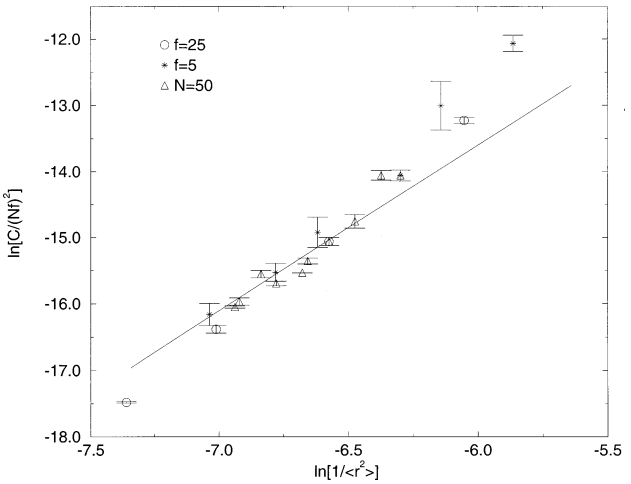

Figure 10. A log−log plot of $C/(Nf)^2$ vs $1/\langle r^2 \rangle$. A solid line of slope $^5/_2$ in included to guide the eye (see eq 5).

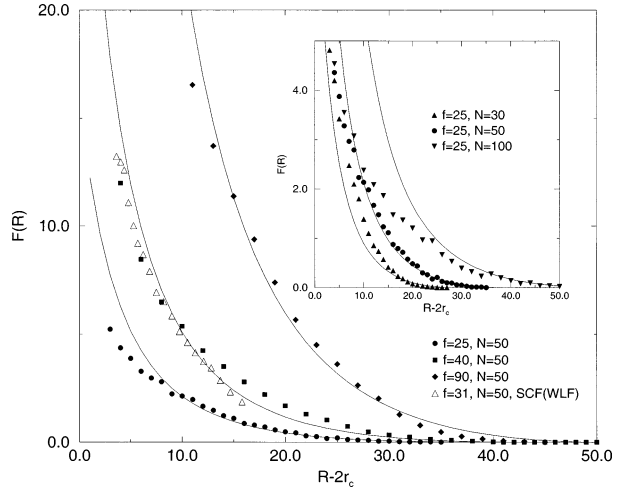

Figure 11. Force between two interacting spherical brushes for a fixed chain length $N = 50$ and differnt number of grafted chains f. Inset plot: force profile for $f = 25$ and different chain lengths. The solid lines correspond to the theoretical predictions of the DL theory. The open triangles in this figure correspond to the force derived by the WLF SCF-lattice model for $f = 31$ and $N = 50$ (taken from ref 35).

the only interaction between them is through the polymer chains, as described by Flory, but as the two brushes approach, the interaction of the chains with the core of the colloidal particle becomes relevant and it is not taken into account.

Next, we compare the computed interacting force between the two brushes with the theoretical predictions of the DL theory. In Figure 11 we show the results for a fixed chain length ($N = 50$) and different number of grafted chains f. We separately represent in the inset plot of the figure the results for $f = 25$ and different polymer lengths. In all the cases studied, systematic deviations from the DL theory are observed at small separating distances between the two brushes. Whereas the DL theory assumes the interacting polymer chains to recoil and keep inside the domain of its own brush V_H, at small distances this requirement cannot be fulfilled together with the excluded-volume criteria; thus, chains are forced to interpenetrate. Besides that, we should note that the DL model is an osmotic model, neglecting the change in the free energy associated with the available chain configurations. DL expected the osmotic term to be much larger in comparison with the configurational one as it happens in planar surfaces. The qualitative agreement found with our Monte Carlo simulations confirms this result for spherical and high grafting densities.

V. Conclusions

In this work we have presented for the first time the results of extensive three-dimensional off-lattice Monte Carlo simulations of two interacting spherical brushes. We have calculated the force for different values of the chain length N and number of grafted chains f. We have found that the force profile can be divided into two regimes. When the brushes are located within a relative close distance, the measured force is well described by the WP theory, whereas as the separation between the brushes increases, the force is reproduced by extending the theory of Flory for dilute polymer solutions. The overall behavior is qualitatively well adjusted, except at short distances, with the phenomenological DL theory for a high density of grafted chains. Finally, we should notice that the characteristic radial size of an isolated brush is found to reproduce the scaling relationship for the star polymer's case.

These results differ from previous numerical studies based on the self-consistent-field lattice formalism of Lind and Gast[34] and Wijmans, Leermakers, and Fleer[35] (to be referred as WLF).

Lin and Gast used a one-dimensional SCF lattice with a modified Derjaguin approximation. Their model could not reproduce the profile predicted by the WP theory, presenting strong discrepancies in systems with large curvature. The main reason is due to the fact that the Dejarguin approximation neglects the lateral distribution of monomers, resulting in an overestimated interacting force.

WLF developed a two-dimensional SCF lattice for an athermal system. Their results for $N = 50$ and $f = 31$, using the same core radius as the one used in our simulations ($r_c = 5$), are reproduced in Figure 11 (open triangles) and compared with our results for $f = 25$ and $f = 40$. Although the results are of the same magnitude, the WLF model overestimates the interaction at short distances. Since the SCF lattice formalism does not account for monomer correlations, there is a higher monomer concentration at short distances in comparison with the one found in Monte Carlo simulations.[36] This higher monomer concentration is responsible for a higher repulsive force.

It is worth commenting that the Flory theory for dilute polymer solutions and the osmotic theory of DL could be also applied to predic the interaction profile for the case of flat grafted layers. In this sense, the Gaussian monomer distribution should be replaced by the characteristic monomer density profile of a flat grafted layer, and a measurement of the typical height of a free brush is also needed.

We expect these results to stimulate further theoretical and experimental studies toward the understanding of more complex systems like the behavior of colloidal particle systems in solution. In this sense, the computed force can be directly related to the measure of disjoint pressures by using the expressions derived by Evans and Napper.[37]

Acknowledgment. We thank A. Chakrabarti for many useful discussions. Financial support from the Ministerio de Ciencia y Tecnologıa (Spain) and FEDER,

Projects BFM2001-0341-C02-01 and BFM2000-1108, is acknowledged.

References and Notes

(1) Napper, D. H. *Polymeric Stabilization of Colloidal Dispersion*; Academic: London, 1983.
(2) Russel, W. B.; Saville, D. A.; Schowalter, W. R. *Colloidal Dispersions*; Cambridge University Press: Cambridge, 1989.
(3) Meyer, R. A. *Appl. Opt.* **1979**, *18*, 585.
(4) van Zanten, J. H.; Monbouquette, H. G. *J. Colloid Interface Sci.* **1991**, *146*, 330.
(5) Hsu, W. P.; Yu, R.; Matijevic, E. *J. Colloid Interface Sci.* **1993**, *156*, 36.
(6) Kuhl, T. L.; Leckband, D. E.; Lasic, D. D.; Israelachvili, J. N. *Biophys. J.* **1994**, *66*, 1479.
(7) de Gennes, P. G. *J. Phys. (Paris)* **1976**, *37*, 1443; *Macromolecules* **1980**, *13*, 1069; *C. R. Acad. Sci. (Paris)* **1985**, *300*, 839.
(8) Alexander, S. *J. Phys. (Paris)* **1977**, *38*, 983.
(9) Semenov, A. N. *Sov. Phys. JETP* **1985**, *61*, 733.
(10) Milner, S. T.; Witten, T. A.; Cates, M. E. *Macromolecules* **1988**, *21*, 2610; *Europhys. Lett.* **1988**, *5*, 413; *Macromolecules* **1989**, *22*, 853.
(11) Milner, S. T.; Witten, T. A. *J. Phys. (Paris)* **1988**, *49*, 1951.
(12) Zhulina, E. B.; Priamitsyn, V. A.; Borisov, O. V. *Polym. Sci. USSR* **1989**, *31*, 205.
(13) Zhulina, E. B.; Borisov, O. V.; Priamitsyn, V. A. *J. Colloid Interface Sci.* **1990**, *137*, 495.
(14) Chakrabarti, A.; Toral, R. *Macromolecules* **1990**, *23*, 2016.
(15) Lai P. Y.; Binder, K. *J. Chem. Phys.* **1991**, *95*, 9288.
(16) Toral, R.; Chakrabarti, A.; Dickman, R. *Phys. Rev. E* **1994**, *50*, 343.
(17) Chakrabarti, A.; Nelson, P.; Toral, R. *Phys. Rev. A* **1992**, *46*, 4930; *J. Chem. Phys.* **1994**, *100*, 748.
(18) Murat, M.; Grest, G. S. *Macromolecules* **1989**, *22*, 4054; *Phys. Rev. Lett.* **1989**, *63*, 1074.
(19) Grant, M. C.; Russel, W. B. *Phys. Rev. E* **1993**, *47*, 2606.
(20) Quirantes, A.; Delgado, A. V. *J. Phys. D: Appl. Phys* **1997**, *30*, 2123.
(21) Phan, S.; Russel, W. B.; Cheng, Z.; Zhu, J.; Chaikin, P. M.; Dunsmuir, J. H.; Ottewill, R. H. *Phys. Rev. E* **1996**, *54*, 6633.
(22) Daoud, M.; Cotton, J. P. *J. Phys. (Paris)* **1982**, *43*, 531.
(23) Witten, T. A.; Pincus, P. A. *Macromolecules* **1986**, *19*, 2509.
(24) Borukhov, I.; Leibler, L. *Phys. Rev. E* **2000**, *62*, R41.
(25) Derjaguin, B. V. *Kolloid Z.* **1934**, *69*, 155.
(26) Toral, R.; Chakrabarti, A. *Phys. Rev. E* **1993**, *47*, 4240.
(27) Nommensen, M. H. G. Duits; van den Ende, D.; Mellema, J. *Phys. Rev. E* **1999**, *59*, 3147.
(28) Flory, P. J. *Principles of Polymer Chemistry*; Cornell University Press: London, 1953.
(29) Doroszkowski, A.; Lambourne, R. *J. Polym. Sci., Part C* **1971**, *34*, 253.
(30) Baungärtner, A. In *Applications of the Monte Carlo Method in Statistical Physics*, 2nd ed.; Binder, K., Ed.; Topics in Current Physics Vol. 36; Springer-Verlag: Berlin, 1987.
(31) Allen, M.; Tildesley, D. *Computer Simulation of Liquids*; Clarendon: Oxford, 1987.
(32) The detailed expressions for the geometrical factors V_R and V_H can be easily obtained as $V_R = {}^1/_3\pi(R_0 - R/2)^2(2R_0 + R/2)$ and $V_H = {}^1/_3\pi(R_0 - R/2)(R_0 + R/2)(R/2) - (2\pi/3)(1 - R/2R_0)\text{-}r_c^3$.
(33) Wijmans, C. M.; Zhulina, E. B. *Macromolecules* **1993**, *26*, 7214.
(34) Lin, E. K.; Gast, A. P. *Macromolecules* **1996**, *29*, 390.
(35) Wijmans, C. M.; Leermakers, F. A. M.; Fleer, G. J. *Langmuir* **1994**, *10*, 4514.
(36) Cosgrove, T.; Heath, T., van Lent, B.; Leermakers, F.; Scheutjens, J. *Macromolecules* **1987**, *20*, 1692.
(37) Evans, R.; Napper, D. H. *J. Colloid Interface Sci.* **1978**, *63*, 43.

MA0213955